2009

Quantitative description of critical current density in YBCO films and multilayers

Alexey V. Pan
University of Wollongong, pan@uow.edu.au

Serhiy Pysarenko
University of Wollongong, serhiy@uow.edu.au

S X. Dou
University of Wollongong, shi@uow.edu.au

Quantitative Description of Critical Current Density in YBCO Films and Multilayers

Alexey V. Pan, Serhiy V. Pysarenko, and Shi X. Dou

***Abstract*—The vortex pinning model based on the presence of the large number of edge dislocations in high quality $YBa_2Cu_3O_7$ (YBCO) films and multilayers has been refined. By introducing the pinning potential of a chain of individual edge dislocations, we have been able not only to describe the critical current density dependence on the applied magnetic field over its entire range, but also to extract the microstructural parameters in the films, such as interdislocation spacing and average domain size, without employing sophisticated microstructural analysis. The model applicability and its results have been verified with the help of microstructural characterization combined with magneto-optical imaging in YBCO films and multilayers with different properties.**

I. Introduction

THE high temperature superconducting (HTS) $YBa_2Cu_3O_7$ (YBCO) or ReBCO films (with Re being rare earth elements) are currently considered as the best materials for HTS wires and cables in the form of so-called coated conductors on flexible metallic templates. Numerous commercial projects and products have already been implemented and are developed. Meanwhile, YBCO films on single crystal substrates and wafers have already been employed for electronic applications, and are explored for broader scope of applications in electronics. On the other hand, an unambiguous understanding and description of the electromagnetic behavior associated with vortex pinning and corresponding structural peculiarities in the films has not been yet achieved.

One of the most successful attempts to describe the critical current density (J_c) as a function of externally applied magnetic field (B_a) has been proposed under the assumption that the YBCO films consists of the network of Josephson junctions (JJs) between grains of the films [1], [2]. However, this assumption can well be accepted for rather granular YBCO films. Indeed, the granularity of YBCO films has been shown to be described by the angle between neighboring grains (domains) in epitaxially grown YBCO films [3]. Films with the angles larger than about 4 ° can be considered to have JJ-like links between the grains. For such films the JJ model should be applicable, and it does describe the $J_c(B_a)$ dependence over the entire magnetic field range [1], [2]. It can be noted that the critical current density degrades exponentially as the angle of the boundaries increases, so that for angles larger than about 4 °, $J_c < 10^{10}$ A/m^2 [3]. For low angle domain boundaries $< 4°$, the critical current density usually reaches values as high as about 0.3 J_0 of the depairing current density (J_0). For these high quality films, the model of JJ between the grains should be rather inappropriate.

Correspondingly, another successful model, working over the entire field range, has been developed [4]. This model is developed on the assumption that the strongest pinning in YBCO films is provided by extended linear defects perpendicular to the superconducting CuO planes, such as edge dislocations. Indeed, columnar-like defects (edge dislocations) with the core size approximately equal to the normal core of vortices in YBCO films [5], [6] provides extremely effective pinning site with strong pinning property [7], [8]. The numerous dislocations in YBCO films grown, for example, by pulsed laser deposition (PLD) or magnetron sputtering (MS) appear due to the mismatch between the crystal lattice parameters of the substrate and the YBCO film. Rows of these dislocations form the network of domain walls [9]–[11]. On one hand, these domain walls are the low angle boundaries between the domains; on the other hand, the individual dislocations forming these walls are the pinning sites for vortices.

In this work, we verify the quantitative model of vortex pining on the dislocations, as well as incorporate the periodic pinning potential of individual dislocations along the domain walls. This is the crucial step in our model as it allows us to (i) "turn on" pinning along the domain walls, preventing slipping vortices along the walls; (ii) make a distinction between high and low quality films, implying low and high angle grain boundaries, as well as clearly granular films having likely JJ-type of contact between the grains; (iii) extract micro- and nano-scale structural parameters without employing sophisticated structural analysis techniques; (iv) describe the $J_c(B_a)$ dependence over the entire field range. One of the most important parameters, which is not yet incorporated in our model, is the influence of the thermally activated processes.

II. Experimental Details

Quality YBCO films and (Y/Nd)BCO multilayers of different thicknesses have been grown by pulsed laser deposition (PLD) with the help of KrF Excimer Laser on (100) $SrTiO_3$ substrates in oxygen atmosphere of 40 Pa [12], and by off-axis DC magnetron sputtering (MS) onto r-cut sapphire (Al_2O_3) buffered with CeO_2 layer [13]. Short samples of YBCO coated conductors (CC) have been also prepared by PLD on the templates provided by THEVA (hastelloy buffered by MgO) and additionally coated by the second $SrTiO_3$ buffer layer [14].

Manuscript received August 26, 2008. First published June 30, 2009; current version published July 15, 2009. This work was supported by the Australian Research Council, as well as by HYPRES Inc. and Mesaplexx Pty Ltd.

The authors are with the Institute for Superconducting and Electronic Materials, University of Wollongong, Northfields Avenue, Wollongong, NSW 2522, Australia (e-mail: pan@uow.edu.au).

Color versions of one or more of the figures in this paper are available online at http://ieeexplore.ieee.org.

Digital Object Identifier 10.1109/TASC.2009.2018265

The surface morphology of the films has been observed by scanning electron microscopy (SEM). Some of the films has been explored at small angles ($\sim 10^{\circ}$ to 20 $^{\circ}$) to the plane of the surface to reveal a more detail surface morphology. Electromagnetic properties of the films have been investigated by magnetization measurements with magnetic fields applied perpendicular to the film planes. $J_c(B_a)$ dependences have been obtained from the width of the magnetization loops, using the critical state model. The magneto-optical (MO) imaging technique has been used to study the local magnetic flux penetration in the YBCO films. This technique is based on the Faraday effect in the MO indicator film (bismuth substituted yttrium iron garnet). The MO images has been taken at a constant temperature after films have been cooled in zero field below the superconducting transition temperature (T_c). The level of brightness in MO images corresponds to the intensity of magnetic flux, so that the brighter the area, the stronger is the flux.

III. Pinning Model

The original pinning model [4] is based on the statistical approach to the pinning of vortices within the domain walls, as the dislocations constituting the walls are considered to be the only existing pinning defects in the films. At very low fields, as only a very few vortices exist in an YBCO film, all the vortices are considered to be pinned. At higher fields, as vortices start forming flux line lattice (FLL) due to intervortex interactions, a number of vortices (n_p) would be still *pinned* within the domain wall pinning bands, whereas the other vortices would be situated outside of the walls (*unpinned* vortices). Thus, we can quantitatively consider the statistics of pinned and unpinned vortices, so that the Lorentz force $f_{\rm L} = J_c\phi_0$ is also equal to $(n_p/n_v)f_p^{\max}$, where ϕ_0 is the flux quantum, n_v is the total number of vortices, and $f_p^{\max}$ is the maximum pinning force.

Considering the rectangular geometry of the structural domains [15] with the dimensions $L_x \times L_y$, we can find the fraction of vortices pinned within the domain wall *pinning* band of $2\delta_c$

$$\frac{n_p(B_a)}{n_v(B_a)} = \int_0^{2\delta_c} W dL_x dL_y + \int_{2\delta_c}^{\infty} W\left[1 - \frac{(L_x - 2\delta_c)(L_y - 2\delta_c)}{L_x L_y}\right] dL_x dL_y \quad (1)$$

where W is the distribution density of the random domain sizes L_x and L_y taken to be a gamma distribution [2] for each dimension. The derivation of this expression is rather straightforward, and it will be published elsewhere [17]. This expression directly leads to the quantitative description of J_c, since $n_p(B_a)/n_v(B_a) = J_c(B_a)/J_c(0)$ with B_a dependence of J_c being encoded in $\delta(B_a, T)$, which is the response of the pinned vortex lattice to the perturbing parameters, such as external field, temperature, current, etc. [8], [17] Since δ_c is the parameter mainly defining the geometry used for the derivation of Eq. (1), it can be substituted with $\delta \leq \delta_c$.

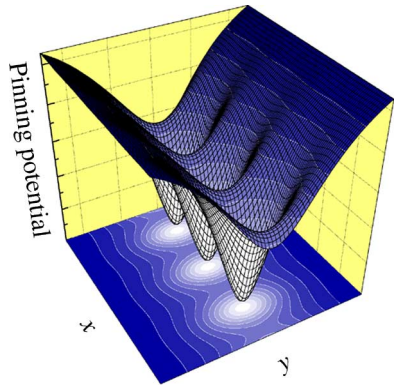

Fig. 1. The pinning potential along a domain boundary, consisting of the equidistantly spaced individual edge dislocations (Eq. (2)). The white lines of the largest superellipses within xy plane indicates the new effective pinning area, which is smaller than the original pinning potential band of the non-modulated grain boundary.

The next important step is to incorporate the pinning property along the domain boundaries. This can be done by taking into account individual edge dislocations with equidistant spacing d between them, situated within (or more exactly along) the boundaries [18] (Fig. 1)

$$\varepsilon_{\rm pin}(x, y) = -\varepsilon_0 \frac{2\pi^2 r_0^2}{d^2\gamma} \frac{\sinh\gamma}{\cosh\gamma - \cos(2\sqrt{2}\pi x/d)} \quad (2)$$

where $\gamma = [(2\sqrt{2}\pi\xi/d)^2 + (2\sqrt{2}\pi y/d)^2]^{1/2}$, $\varepsilon_0 = [\phi_0/(4\mu_0\pi\lambda)]^2$ is the flux line energy, ξ is the temperature dependent coherence length, μ_0 is the permeability of free space, and r_0 is the radius of a normal dislocation core. Taking into account the reduced area of the $2\delta_c$ pinning band along the boundary (the dotted line in the xy plane in Fig. 1), which individually can be well approximated by a superellipse, we can find a geometrical coefficient $K_{\rm sh}(d, \delta_c)$

$$K_{\rm sh} = \frac{\delta_c \int_0^{d/2} (1 - (x/\delta_c)^m)^{1/n}\, dx}{\delta_c(d/2)} \quad (3)$$

Finally, multiplying Eq. (1) by the coefficient Eq. (3), we obtain the expression for the $J_c(B_a)/J_c(0)$, which is used for fitting our experimental curves (a more detailed derivation will be published elsewhere [17]). Note, that this expression contain the structural parameters of the films: the interdislocation spacing d, the average domain size $\langle L\rangle = \langle L_x\rangle = \langle L_y\rangle$, and the distribution for the domain sizes (introduced via W and reflected in parameter ν [2]).

IV. Analysis of Different YBCO Films

In Fig. 2, we show four surface landscapes of four different YBCO films obtained by SEM. The surface of a 300 nm thick PLD film is shown in (a), of a 1000 nm thick (Y/Nd)BCO multilayer [12] in (b), of a 300 nm thick MS film with some ab-growth (rectangular blocks) in (c), and of a 3600 nm thick coated conductor (CC) in (d). A granular structure with strongly

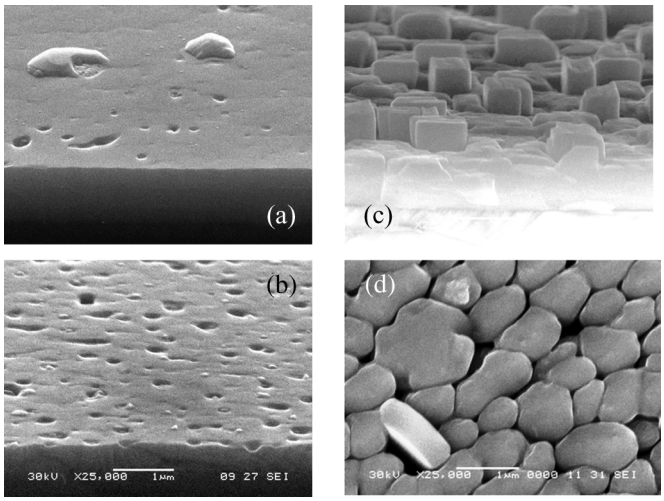

Fig. 2. SEM images of the surfaces in (a) the PLD film, (b) the multilayer, (c) the MS film with ab-growth (rectangular blocks on the surface), (d) the CC film. The scale is the same for all images.

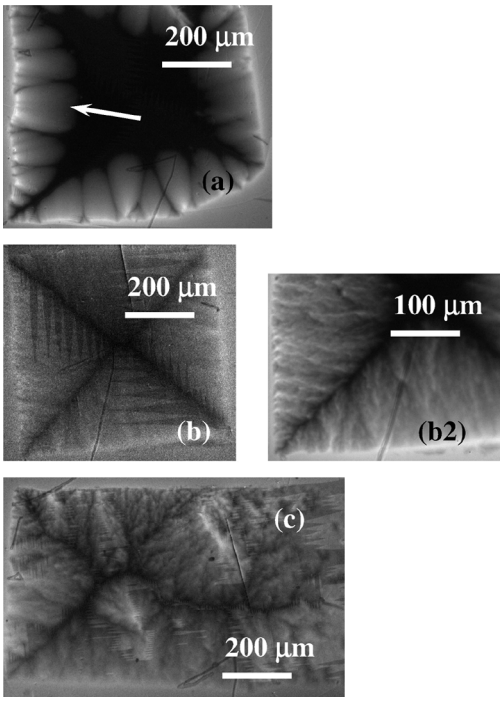

Fig. 3. Magneto-optical (MO) images of the magnetic flux penetration in (a) the PLD film, (b) the MS film, and (c) the CC film. For the MS film, the magnification is also shown in (b2) to better visualize the uneven flux penetration in this film. The white arrow points out the smooth flux front between defects at the edge of the film.

pronounced grain boundaries can be readily recognized for the CC film in (d). In the case of the MS film with ab-blocks on the surface (c), grain boundaries might be also assumed along the ab-blocks boundaries. In the PLD film and the multilayer, a granular (or misoriented domain) structure is not visible in the SEM images (a) and (b).

In Fig. 3, it is seen that the conclusion on granularity made on the basis of the surface structures is supported by the MO images of the magnetic flux penetration into the films investigated. The flux front penetration is very smooth [white arrow

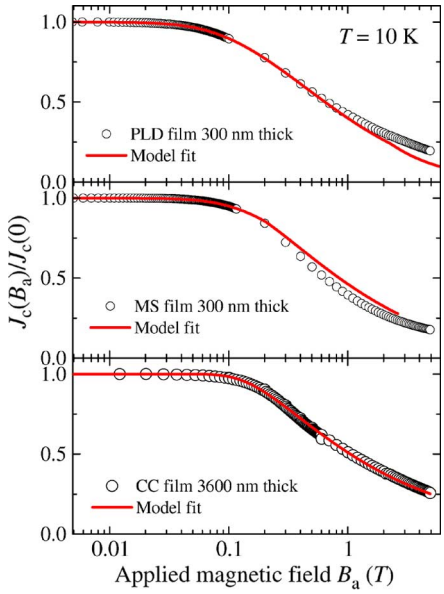

Fig. 4. The critical current density as a function of the applied field for (top) the PLD film, (middle) the MS film, and (bottom) the CC film with the corresponding fits (solid lines) obtained within the model developed as described in the text.

in Fig. 3(a)] for the PLD film and the multilayer (the multilayer is not shown as it is very similar to PLD film), apart from the irregularities associated with defects at edges of the films. Generally, the brighter is the area, the stronger the magnetic flux intensity is. The flux penetration into the CC film is extremely irregular [Fig. 3(c)], which is likely due to the enhanced penetration along the grain boundaries and rather strong screening within individual grains. The penetration along the boundaries indicates weak (or absence of) pinning along the boundaries. In the case of the MS film [Fig. 3(b)], the inhomogeneity of the flux penetration can be recognized at a higher magnification [Fig. 3(b2)]. It is likely that a rather homogeneous flux penetration in the film is overlapped with an additional penetration associated with the ab-oriented grains. Indeed, SEM images taken at an angle of about 30 ° to the plane of the surface [Fig. 2(c)] show that ab-grains are usually initiated not at the interface with the substrate, but at a certain thickness above the interface. This situation results in the enhanced penetration along ab-grain boundaries being "smeared" by the smooth flux penetration in the lower part of the film with presumably only slightly misoriented domains near the interface.

The situation in the films investigated is further clarified by fitting experimental $J_c(B_a)$ curves (Fig. 4) with the product of two expressions Eqs. (1) and (3) as derived within our model (see the last paragraph in Section III). Even more importantly, the consistency of the structural, MO, and fitting results also proves that our approach to pinning and $J_c(B_a)$ descriptions works well and robustly with films possessing different microstructures and correspondingly expected to have different pinning properties. As the fitting results are similar for our PLD films and multilayers, we show three $J_c(B_a)$ curves with the corresponding fits (solid lines) for the PLD (top), MS (middle), and CC (bottom) films. The corresponding structural parameters obtained from fitting are as follows. For the PLD

film, we get $d = 32$ nm, $\langle L \rangle = 272$ nm, and $\nu = 1.67$; for the MS film: $d = 28$ nm, $\langle L \rangle = 244$ nm, and $\nu = 2.08$; for the CC film: $d = 75$ nm, $\langle L \rangle = 276$ nm, and $\nu = 14$. As a simple comparison, the average size of grains was found to be 200 nm in 140 nm thick film [16]. Clearly, the size of grains is affected by the method of deposition, deposition parameters, and the thickness of samples.

In the case of the CC film, the domain size distribution parameter ν is very large and in fact becomes hardly sensitive to the fitting procedure for its even larger values, which also casts some doubts on the validity of applying our model (including the results for d and $\langle L \rangle$) for this film. In addition, the fitting curve in Fig. 4 (bottom) does not fit the data to the required accuracy in the intermediate field range (the fitting curve deviates notably from the centers of the experimental data circles), compared to the other films. Under the intermediate field range we imply the range at and just below the transition from the field-independent J_c to the field-dependent J_c region, in which the model works the most effectively [17]. At higher fields, the contribution from other pinning sources (other than linear defects) and particularly thermal activations, which are not taken into account in the model, starts influencing the experimental behavior. As a result, the fitting procedure works much worse at high fields and temperatures (which is also a strong indication of the credibility of our model). This fitting result, combined with the SEM observations of the granularity and the MO imaging of the irregular flux penetration in the CC film, points out that this film is unlikely can be described by the edge dislocation pinning model derived. A more appropriate model for description of this film might be the JJ-like contacts between grains [1], [2].

As to the other films, it can be seen that in spite of the different surface structure a similar results are obtained. However, the MS film shows smaller distance d between dislocations, which indicate a larger misorientation angle between the domains than in the PLD film; the average domain size $\langle L \rangle$ is smaller; and the domain size distribution ν is broader (a larger value of ν). These results well correspond to the differences in SEM observations and MO imaging for these films.

V. Conclusion

In conclusion, the model of vortex pinning on dislocations has been substantially revised, and the pinning potential of an infinite chain of individual edge dislocations with normal cores has been successfully incorporated into the model. The model, describing $J_c(B_a)$ over the entire field range, generates the microstructural parameters, such as the average spacing between the individual dislocations (which allows to easily determine the misorientation angle between the domains), average size of the domains in the films, and the domain size distribution. The derived model is verified to work on various films with different microstructural and electromagnetic properties. Extracted structural parameters coincide with those obtained in structural analysis experiments [4], [17] and those determined by a different approach described in Refs. [19], [20]. The results of this work indicate that the expensive and time-consuming structural analysis, such as transmission electron microscopy, can be substituted by the fitting procedure developed within the model.

References

[1] E. Mezzetti, R. Gerbaldo, G. Ghigo, L. Gozzelino, B. Minetti, C. Camerlingo, A. Monaco, G. Cuttone, and A. Rovelli, *Phys. Rev. B*, vol. 60, p. 7623, 1999.

[2] G. Ghigo, A. Chiodoni, R. Gerbaldo, L. Gozzelino, E. Mezzetti, B. Minetti, C. Camerlingo, G. Cuttone, and A. Rovelli, *Supercond. Sci. Technol.*, vol. 12, p. 1059, 1999.

[3] H. Hilgenkamp and J. Mannhart, "Grain boundaries in high- T_c superconductors," *Rev. Mod. Phys.*, vol. 74, p. 485, 2002.

[4] V. Pan, Y. Cherpak, V. Komashko, S. Pozigun, C. Tretiatchenko, A. Semenov, E. Pashitskii, and A. V. Pan, "Supercurrent transport in $YBa_2Cu_3O_{7-\delta}$ epitaxial thin films in a dc magnetic field," *Phys. Rev. B*, vol. 73, p. 054508, 2006.

[5] A. Gurevich and E. A. Pashitskii, *Phys. Rev. B*, vol. 57, p. 13878, 1998.

[6] V. M. Pan and A. V. Pan, "Vortex matter in superconductors," *Low Temp. Phys.*, vol. 27, pp. 732–746, 2001.

[7] L. Krusin-Elbaum, L. Civale, G. Blatter, A. D. Marwick, F. Holtzberg, and C. Field, *Phys. Rev. Lett.*, vol. 72, p. 1914, 1994.

[8] G. Blatter, M. V. Feigel'man, V. B. Geshkenbein, A. I. Larkin, and V. M. Vinokur, "Vortices in high-temperature superconductors," *Rev. Mod. Phys.*, vol. 66, p. 1125, 1994.

[9] V. M. Pan, A. L. Kasatkin, V. L. Svetchnikov, and H. W. Zandbergen, *Cryogenics*, vol. 33, p. 21, 1993.

[10] Y. V. Fedotov, S. M. Ryabchenko, E. A. Pashitskii, A. V. Semenov, V. I. Vakaryuk, V. M. Pan, and V. S. Flis, *Low Temp. Phys.*, vol. 28, p. 172, 2001.

[11] Y. V. Fedotov, S. M. Ryabchenko, E. A. Pashitskii, A. V. Semenov, V. I. Vakaryuk, V. M. Pan, and V. S. Flis, *Fiz. Nizk. Temp.*, vol. 28, pp. 245–261, 2002.

[12] A. V. Pan, S. Pysarenko, and S. X. Dou, "Drastic improvement of surface structure and current-carrying ability in $YBa_2Cu_3O_7$ films by introducing multilayered structure," *Appl. Phys. Lett.*, vol. 88, p. 232506, 2006.

[13] D. A. Luzhbin, A. V. Pan, V. A. Komashko, V. S. Flis, V. M. Pan, S. X. Dou, and P. Esquinazi, "Origin of paramagnetic magnetization in field-cooled $YBa_2Cu_3O_{7-\delta}$ films," *Phys. Rev. B*, vol. 69, p. 024506, 2004.

[14] S. V. Pysarenko, A. V. Pan, and S. X. Dou, "Development of multilayer coated conductors with simplified buffer architectures," in *International Conference on Electronic Materials (IUMRS-ICEM08)*, Sydney, Australia, July 28–August 1 2008.

[15] V. Svetchnikov, V. Pan, C. Traeholt, and H. Zandbergen, *IEEE Trans. Appl. Supercond.*, vol. 7, p. 1396, 1997.

[16] F. C. Klaassen, G. Doornbos, J. M. Huijbregtse, R. C. F. van der Geest, B. Dam, and R. Griessen, "Vortex pinning by natural linear defects in thin films of $YBa_2Cu_3O_{7-\delta}$," *Phys. Rev. B*, vol. 64, p. 184523, 2001.

[17] A. V. Pan and S. V. Pysarenko, . : , unpublished.

[18] E. A. Pashitskii and V. I. Vakaryuk, *Low Temp. Phys.*, vol. 28, p. 11, 2002.

[19] A. V. Pan and S. X. Dou, "Comparison of small-field behavior in MgB_2, low- and high-temperature superconductors," *Phys. Rev. B*, vol. 73, p. 052506, 2006.

[20] A. V. Pan *et al.*, "Thermally activated depinning of individual vortices in $YBa_2Cu_3O_7$ superconducting films," *Physica C*, vol. 407, pp. 10–16, 2004.